Nano World Journal

https://doi.org/10.17756/nwj.2023-s1-090

Research Article

Open Access

Comparative Study of Impact Behavior of Fused Filament Fabrication-printed Polylactic Acid Composites

Akash Jain, Sushil Kumar, Abhishek Singh, Ankit Sahai* and Rahul Swarup Sharma

3D Printing and Additive Manufacturing Lab, Department of Mechanical Engineering, Dayalbagh Educational Institute, Dayalbagh, Agra, Uttar Pradesh, India

***Correspondence to:**
Ankit Sahai
3D Printing and Additive Manufacturing Lab,
Department of Mechanical Engineering,
Dayalbagh Educational Institute,
Dayalbagh, Agra, Uttar Pradesh, India.
E-mail: sahaiankit@dei.ac.in

Received: November 24, 2022
Accepted: April 23, 2023
Published: April 25, 2023

Citation: Jain A, Kumar S, Singh A, Sahai A, Sharma RS 2023. Comparative Study of Impact Behavior of Fused Filament Fabrication-printed Polylactic Acid Composites. *NanoWorld J* 9(S1): S470-S475.

Published by United Scientific Group

Abstract

Fused Filament Fabrication (FFF) is a frequently utilised Additive Manufacturing (AM) method, because of its low equipment costs and user-friendliness. Carbon-based reinforcements including carbon fibres, graphene, and multi-walled carbon nano tubes can be used to increase impact resistance of polylactic acid (PLA) and therefore its applicability in dissimilar fields. In this work, FFF process is used to analyse and compare the impact properties of three different types of reinforced PLA composites made from carbon fibre, graphene, and multi-walled carbon nano tubes. Energy absorption and impact strength (IS) are studied in relation to the selected process parameters, which include raster orientation (0°, 45°, and 90°), feed rate (20 mm/s, 40 mm/s, and 60 mm/s), and layer thickness (0.10 mm, 0.15 mm, and 0.20 mm). The morphology of failure in specimens can also be studied with high-end microscopy. Using ANOVA (Analysis of Variance) and Taguchi methods, the data analysis is performed for the dependency of IS on the selected process parameters and find that the raster orientation and layer thickness have the principal influence on IS, followed by the filament material and feed rate. Maximum IS of the specimen is 29.980 kJ/m^2 at 0.20 mm layer height, 45° raster orientation, and 20 mm/s feed rate for carbon fibre reinforcement.

Keywords

Impact strength, Reinforcement, Failure morphology, Polylactic acid, Fused filament fabrication

Introduction

Extremely durable materials are needed for numerous uses, and this includes withstanding impacts. AM is a more efficient and affordable method of constructing complex geometries that lead to individualised functional designs [1]. FFF provides low upfront costs, wide availability of materials, and ease of usage [2, 3]. In the FFF technique, the part is manufactured layer by layer by extruding polymer filament via a hot nozzle and depositing it on the build platform [4]. Important factors to think about in the FFF process are raster orientation, layer thickness, build orientation, and raster width [5, 6]. The material's tensile, flexural, and impact properties were all found to be significantly affected by these factors [7]. Additionally, while a small number of research [8, 9] have looked at optimising processing parameters to improve the mechanical characteristics of thermoplastic components, the properties of produced parts through FFF are intrinsically poor. The impact testing specimen for the Izod pendulum impact resistance test is a standardised size that meets the requirements of ASTM D256 [3, 10]. As the hammer is raised, it is dropped from a predetermined height. As it comes to rest, the hammer strikes a specimen that has been notched. The IS is determined by the amount of energy that can withstand an impact [11,

12]. Due to its high inflexibility, high mechanical properties, convenience of usage, and most significantly, biodegradability [13], PLA stands out as the most promising of the materials studied. Some industries are still wary of using PLA because of its low impact and thermal resistance [14]. Many studies were undertaken to increase PLA's resistance to impact, and they were successful after the material was reinforced with carbon fibres, graphene, and multi-walled carbon nanotubes. High alignment between the direction of material deposition and the orientation of carbon fibres in the PLA composite was reported to improve mechanical performance [15-17].

The current work examines how different reinforcement and process factors affect the mechanical behaviour of specimens by manipulating RO (raster orientation), FR (feed rate), and LT (layer thickness) for selected PLA composites. To get insight into the root reasons of failure, micrography imaging is performed for the deformed surfaces. The impact test data is examined with ANOVA and Taguchi methods to learn how different process parameters affect the mechanical features.

Materials and Methods

In FFF, solid shapes are created using a material extrusion technique. Filaments of 1.75 mm in diameter are used, each made of C-PLA (carbon fibre 20% by weight), G-PLA (graphene 20% by weight), and M-PLA (multi-walled carbon nano tubes 20% by weight). The specimen was formed with a 0.4 mm nozzle diameter on a CUB 5.5 3D printer. The specimen was designed in Simplify3D and SolidWorks 2019. For the purpose of observing the effects of varying RO, FR, and LT on impact testing results, specimens were manufactured in accordance with ASTM D256 (Figure 1). Variations in the following process parameters are used to create the 27 different specimens using RO (0°, 45°, and 90°), FR (20 mm/s, 40 mm/s, and 60 mm/s), and LT (0.1 mm, 0.15 mm, and 0.2 mm). Table 1 illustrates the utilized process parameters.

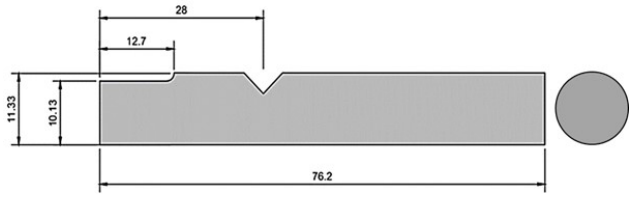

Figure 1: Impact test specimen with dimensions.

Following tensile testing, the data (Table 2) is analysed to determine the best three specimens exhibit the higher tensile strength for at a given LT. Therefore, subsequent impact test specimens with the selected filament materials, are made based on the selection of nine different process parameter combinations. The samples were subjected to impact testing. The process parameters and the materials used in the fabrication are examined and compared for their impact behaviour. The IS and Energy Absorbed of the impact test specimen, figure 2, are described in table 3.

(a) (b) (c)

Figure 2: Tested impact test specimen **(a)** C-PLA, **(b)** G-PLA, and **(c)** M-PLA.

Results and Discussion

The total number of specimens used for individual process parameter combination is shown in table 2; this includes C-PLA as the material being fabricated and a selected range of RA, FR, and LT values. As seen in figure 3, C-PLA samples experience a wide range of stress and strain.

Maximum tensile strength for C-PLA was measured at 25.189 MPa with 1.618% elongation at break, and minimum tensile strength was measured at 16.511 MPa with 0.659% elongation at break. Accordingly, by manipulating the parameters, a 52.56% increase in tensile strength is achieved. Using nine specified process variables (Table 3) and selected fabricating materials, figure 4 depicts the results of impact testing.

Effect of raster orientation

Finding demonstrates that the IS decreases as the RO is increased from 0° to 90°. For C-PLA, IS at FR 20 mm/s and LT 0.10 mm is improved by 21.43%, from 17.488 kJ/m^2 (C-2)

Table 1: Process parameters of FFF process.

Fixed process parameters			Variable process parameters		
Parameters	**Value**	**Unit**	**Parameters**	**Values**	**Unit**
Infill pattern	Rectilinear	-	Raster Orientation	0, 45, 90	°
Build Orientation	XY	-	Feed Rate	20, 40, 60	mm/s
Infill density	80	%	Layer Thickness	0.10, 0.15, 0.20	mm
Liquefier temperature	210	°C			
Bed temperature	60	°C			

Table 2: Tensile test results for tensile specimens.

Specimen Code	LT	FR	RO	Tensile Strength	Modulus	Elongation at Break	Selected Parameters
	(mm)	(mm/s)	(°)	(MPa)	(GPa)	(%)	
S1	0.10	20	0	25.189	4.371	1.618	1
S2			45	22.954	4.135	0.169	2
S3			90	21.918	3.764	0.343	-
S4		40	0	21.862	3.823	0.826	-
S5			45	20.824	3.938	0.425	-
S6			90	22.813	3.518	1.054	-
S7		60	0	23.146	3.639	1.352	3
S8			45	22.418	3.871	0.793	-
S9			90	20.523	4.294	0.557	-
S10	0.15	20	0	24.626	3.737	1.302	4
S11			45	20.357	4.193	0.644	-
S12			90	20.723	3.937	0.898	-
S13		40	0	23.374	4.198	0.536	5
S14			45	18.968	3.859	0.447	-
S15			90	20.393	4.223	0.357	-
S16		60	0	19.439	3.191	0.525	-
S17			45	20.856	4.269	0.399	-
S18			90	21.786	3.785	0.013	6
S19	0.20	20	0	19.614	4.223	0.577	-
S20			45	22.977	3.451	1.186	7
S21			90	18.425	3.144	0.842	-
S22		40	0	22.873	3.745	1.396	8
S23			45	16.511	3.213	0.659	-
S24			90	18.599	3.155	1.119	-
S25		60	0	22.858	3.686	1.137	9
S26			45	16.617	3.234	0.168	-
S27			90	16.579	3.421	0.389	-

to 21.236 kJ/m^2 (C-1), when the RO is changed from 45° to 0°. The IS of G-PLA is improved by 50.00% when the RO is changed from 45° to 0°, from 12.492 kJ/m^2 (G-2) to 18.738 kJ/m^2 (G-1). These values are based on an LT of 0.10 mm and a FR of 20 mm/s. The IS of M-PLA is increased by 41.67% when the RO is changed from 45° to 0°, from 14.990 kJ/m^2 (M-2) to 21.236 kJ/m^2 (M-1) at LT of 0.10 mm and a FR of 20 mm/s. At constant conditions, the specimen built with RO 0° provides higher impact resistance because to the robust interlayer bonding and its perpendicular orientation of the raster's. The peak IS attained at a RO of 0°, and it diminishes with increasing RO.

Effect of layer thickness

Increasing the LT from 0.10 mm to 0.20 mm improve IS. For C-PLA, by increasing the LT from 0.15 mm to 0.20 mm, the IS at RO 0° and FR 40 mm/s is enhanced by 18.75%, from 19.987 kJ/m^2 (C-5) to 23.734 kJ/m^2 (C-8). Increasing the LT from 0.10 mm to 0.20 mm increases the IS of G-PLA from 12.492 kJ/m^2 (G-2) to 27.482 kJ/m^2 (G-7) when subjected to a RO of 45° and a FR of 20 mm/s. By increasing the LT from 0.10 mm to 0.15 mm, the IS of M-PLA is increased by 18.75%, from 21.236 kJ/m^2 (M-1) to 27.482 kJ/m^2 (M-4) at RO 0° and FR 20 mm/s. It's possible that this is due to the fact that a thicker layer provides better protection against impact blows, and that the more heat stored by a thicker raster encourages raster bonding, leading to greater overall strength.

Effect of feed rate

It has been noticed that as the FR is increased from 20

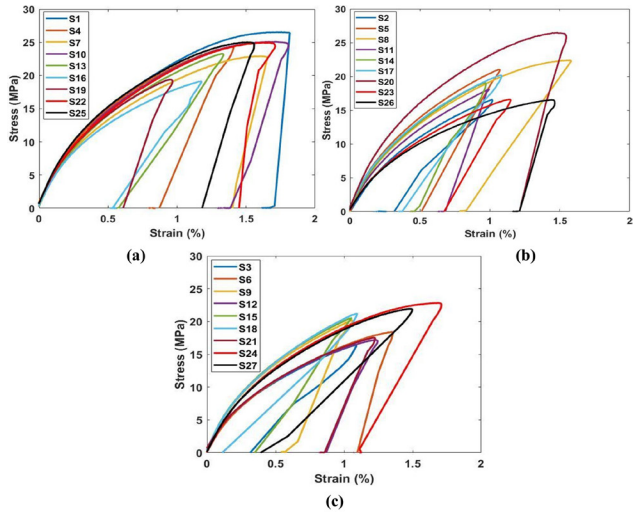

Figure 3: Stress strain variation for tensile specimens **(a)** at RO 0°, **(b)** at RO 45°, and **(c)** at RO 90°.

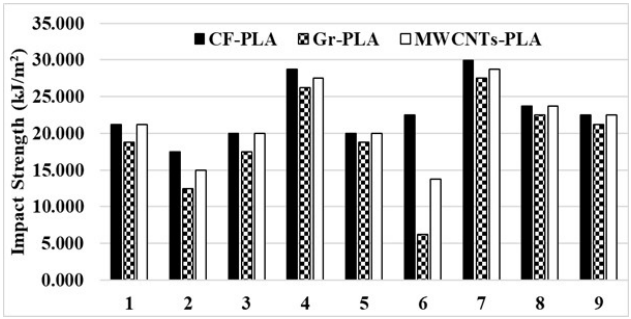

Figure 4: Variation of IS for different specimens.

mm/s to 60 mm/s, the IS falls. At RO 0° and LT 0.15 mm, reducing the FR from 40 mm/s to 20 mm/s increases the IS of C-PLA by 27.78%, from 22.485 kJ/m² (C-5) to 28.731 kJ/m² (C-4). If the FR is lowered from 60 mm/s to 20 mm/s, the IS of G-PLA at RO 0° and LT 0.10 mm increases by 7.15%, from 17.488 kJ/m² (G-3) to 18.738 kJ/m² (G-1). If the FR is decreased from 60 mm/s to 40 mm/s, the IS at RO 0° and LT 0.20 mm increases by 5.55%, from 22.485 kJ/m² (M-9) to 23.734 kJ/m² (M-8) for M-PLA. With the same RO and LT, a higher FR has a lower IS. An increase in FR could be the best choice if you need to print more quickly at the expense of some IS.

Failure morphology

Maximum IS of G-PLA was found to be 27.482 kJ/m² (G-7) at RO 45°, FR 20 mm/s, and LT 0.2 mm, while maximum IS of M-PLA was found to be 28.731 kJ/m² under the same conditions (M-7). When compared to G-PLA and M-PLA, C-PLA shows a maximum IS of 29.980 kJ/m² (C-7), which is 9.09% and 4.35% greater, respectively. It is evident from the micrographs, figure 5, that G-PLA has a lower IS because to the increased number of voids. Weak raster-to-raster bonding is the primary reason for specimen failure for M-PLA. The IS and durability of a material decreases as the number of connecting lines and voids increases. C-PLA displays the maximum IS since each raster bears the impact force before failure.

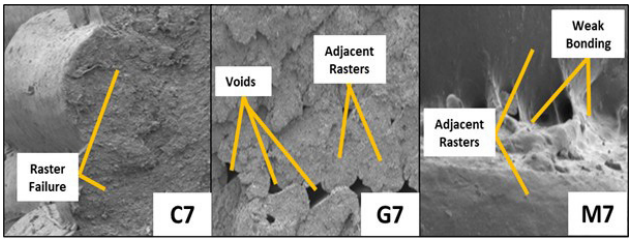

Figure 5: Deformed surface of the selected impact test specimens.

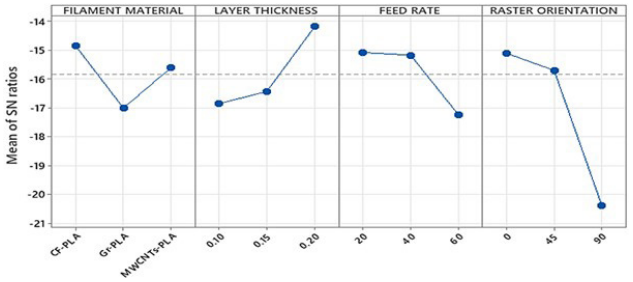

Figure 6: SN ratios plots of the main effects of the process parameters on the IS of the specimens.

Analysis of Variance

Greater is better in the main effects plot for signal-to-noise ratios (SN ratios), figure 6, from ANOVA with Taguchi Method analysis of the selected process parameters, and Filament Material over the target factor utilizing the MINITAB 21 software.

Table 4 illustrates the contribution levels for the selected parameters. The P-value indicates that RO and LT have a significant impact on IS, followed by filament material and FR, with an R^2 for IS of 72.73%.

Conclusions

The determination of this study was to examine the effects that changing the process parameters RO, FR, and LT had on the mechanical behaviour of FFF-fabricated C-PLA, G-PLA, and M-PLA specimens. The best material-parameter combinations for enhanced IS are outlined in this paper. The specimen C7 exhibited the highest IS of 29.980 kJ/m², which corresponds to C-PLA as filament material at LT 0.20 mm, RO 45°, and FR 20 mm/s. It is found from the experimental results that when the LT increases, the IS of the specimens increases but decreases with the increment in RO and FR. Based on P-values, it can be concluded that the IS is mainly influenced by the RO and LT, followed by FR and filament material.

Acknowledgments

TFractography analysis was performed at DEI's FESEM lab in the Department of Chemistry, for which the authors express gratitude. We are also thankful to the grant received from AICTE (file no. 8-88/FDC/RPS (POLICY-1)/ 2019-20).

Table 3: Impact test results.

Specimen Code	Filament Material	LT (mm)	FR (mm/s)	RO (°)	Energy Absorbed (kg-m)	IS (kJ/m²)
C-1	C-PLA	0.1	20	0	0.17	21.236
C-2			20	45	0.14	17.488
C-3			60	0	0.16	19.987
C-4		0.15	20	0	0.23	28.731
C-5			40	0	0.16	19.987
C-6			60	90	0.18	22.485
C-7		0.2	20	45	0.24	29.980
C-8			40	0	0.19	23.734
C-9			60	0	0.18	22.485
G-1	G-PLA	0.1	20	0	0.15	18.738
G-2			20	45	0.10	12.492
G-3			60	0	0.14	17.488
G-4		0.15	20	0	0.21	26.233
G-5			40	0	0.15	18.738
G-6			60	90	0.05	6.246
G-7		0.2	20	45	0.22	27.482
G-8			40	0	0.18	22.485
G-9			60	0	0.17	21.236
M-1	M-PLA	0.1	20	0	0.17	21.236
M-2			20	45	0.12	14.990
M-3			60	0	0.16	19.987
M-4		0.15	20	0	0.22	27.482
M-5			40	0	0.16	19.987
M-6			60	90	0.11	13.741
M-7		0.2	20	45	0.23	28.731
M-8			40	0	0.19	23.734
M-9			60	0	0.18	22.485

Table 4: ANOVA for impact test specimens.

Source	DF	Seq SS	Adj SS	Adj MS	F	P	Contribution
Filament Material	2	21.47	21.47	10.737	3.6	0.05	11.06%
Layer Thickness	2	37.13	47.24	23.621	7.8	0	24.34%
Feed Rate	2	30.99	15.96	7.982	2.7	0.1	8.22%
Raster Orientation	2	55.12	55.12	27.559	9.1	0	28.40%
Residual Error	18	54.27	54.27	3.015	-	-	27.97%
Total	26	198.98	-	-	-	-	-
S = 1.7363, R^2 = 72.73%, and R^2 (Adj) = 60.61%							

Conflict of Interest

The authors declared no potential conflict of interest for this article.

References

1. Scrocco M, Chamberlain T, Chow C, Weinreber L, Elks E, et al. 2018. Impact testing of 3D printed kevlar-reinforced onyx material. In International Solid Freeform Fabrication Symposium. University of Texas, Austin, United States.
2. Tezel T, Ozenc M, Kovan V. 2021. Impact properties of 3D-printed engineering polymers. *Mater Today Commun* 26: 102161. https://doi.org/10.1016/j.mtcomm.2021.102161
3. Pushpandhini S, Surendran R. 2021. Experimental testing of PLA material using fused deposition modeling. *Int Res J Eng Technol* 8(3): 1088-1094.
4. Rajpurohit SR, Dave HK. 2021. Impact strength of 3D printed PLA using open source FFF-based 3D printer. *Prog Addit Manuf* 6(1): 119-131. https://doi.org/10.1007/s40964-020-00150-6
5. Kain S, Ecker JV, Haider A, Musso M, Petutschnigg A. 2020. Effects of the infill pattern on mechanical properties of fused layer modeling (FLM) 3D printed wood/polylactic acid (PLA) composites. *Eur J Wood Prod* 78: 65-74. https://doi.org/10.1007/s00107-019-01473-0
6. Yadav P, Sahai A, Sharma RS. 2019. Experimental Investigations for Effects of Raster Orientation and Infill Design on Mechanical Properties in Additive Manufacturing by Fused Deposition Modelling. In Narayanan R, Joshi S, Dixit U (eds) Advances in Computational Methods in Manufacturing. Lecture Notes on Multidisciplinary Industrial Engineering. Springer, Singapore, pp 415-424.
7. Naik M, Thakur DG. 2021. Experimental investigation of effect of printing parameters on impact strength of the bio-inspired 3D printed specimen. *Sādhanā* 46(3): 151. https://doi.org/10.1007/s12046-021-01671-8
8. Caminero MÁ, Chacón JM, García-Plaza E, Núñez PJ, Reverte JM, et al. 2019. Additive manufacturing of PLA-based composites using fused filament fabrication: effect of graphene nanoplatelet reinforcement on mechanical properties, dimensional accuracy and texture. *Polymers* 11(5): 799. https://doi.org/10.3390/polym11050799
9. Yadav P, Sahai A, Sharma RS. 2021. Flexural strength and surface profiling of carbon-based PLA parts by additive manufacturing. *J Inst Eng India Ser C* 102(4): 921-931. https://doi.org/10.1007/s40032-021-00719-2
10. Shahar FS, Sultan MTH, Safri SNA, Jawaid M, Talib ARA, et al. 2022. Fatigue and impact properties of 3D printed PLA reinforced with kenaf particles. *J Mater Res Technol* 16: 461-470. https://doi.org/10.1016/j.jmrt.2021.12.023
11. Gong H, Xing X, Nel J. 2019. Impact strength of 3D printed polyether-ether-ketone (PEEK). In International Solid Freeform Fabrication Symposium. University of Texas, Austin, United States.
12. Wang L, Gramlich WM, Gardner DJ. 2017. Improving the impact strength of Poly (lactic acid) (PLA) in fused layer modeling (FLM). *Polymer* 114: 242-248. https://doi.org/10.1016/j.polymer.2017.03.011
13. Yadav P, Sahai A, Sharma RS. 2021. Strength and surface characteristics of FDM-based 3D printed PLA parts for multiple infill design patterns. *J Inst Eng India Ser C* 102: 197-207. https://doi.org/10.1007/s40032-020-00625-z
14. Camargo JC, Machado ÁR, Almeida EC, Silva EFMS. 2019. Mechanical properties of PLA-graphene filament for FDM 3D printing. *Int J Adv Manuf Technol* 103: 2423-2443. https://doi.org/10.1007/s00170-019-03532-5
15. Yadav P, Sahai A, Sharma RS. 2022. Experimental studies on the mechanical behaviour of three-dimensional PLA printed parts by fused filament fabrication. *J Inst Eng India Ser D* 1-13. https://doi.org/10.1007/s40033-022-00403-4
16. Ansari AA, Kamil M. 2022. Izod impact and hardness properties of 3D printed lightweight CF-reinforced PLA composites using design of experiment. *Int J Lightweight Mater Manuf* 5(3): 369-383. https://doi.org/10.1016/j.ijlmm.2022.04.006
17. Jain A, Mishra A, Dubey AK, Kumar A, Sahai A, et al. 2022. Mechanical characteristics and failure morphology of FFF-printed poly lactic acid composites reinforced with carbon fibre, graphene and MWCNTs. *J Thermoplast Compos Mater*. https://doi.org/10.1177/08927057221133089